COMPARISON OF TECTONIC FEATURE LOCATIONS AND CRUSTAL THICKNESS IN THE NORTHERN HEMISPHERE OF MERCURY. Michelle M. Selvans[1], Thomas R. Watters[1], Peter B. James[2], Maria T. Zuber[2], and Sean C. Solomon[3], [1]Center for Earth and Planetary Studies, National Air and Space Museum, Smithsonian Institution, Washington, DC 20560, USA (selvansm@si.edu); [2]Department of Earth, Atmospheric and Planetary Sciences, Massachusetts Institute of Technology, Cambridge, MA 02139, USA; [3]Lamont-Doherty Earth Observatory, Columbia University, Palisades, NY 10964, USA.

Introduction: Interior cooling and the resultant radial contraction of Mercury dominated the contribution to the contractional strain expressed by lobate scarps and high-relief ridges [1, 2]. The underlying large thrust faults should be randomly distributed over the surface if their formation was purely the result of global contraction, but instead these features appear to be concentrated in some regions and relatively deficient in others [3–5]. We therefore ask the questions: What combination of stresses caused lobate scarps and high-relief ridges to form at the locations and orientations observed? Was mantle convection partly responsible for concentrating tectonic features? Here we address the latter question in particular.

Background: The origin and distribution of contractional features have been addressed with Mariner 10 images and models of mantle convection [e.g., 3, 6]. We follow up on those studies with data from the MErcury Surface, Space ENvironment, GEochemistry, and Ranging (MESSENGER) mission [7]. Orbital imaging campaigns allow for the most accurate mapping of lobate scarps and high-relief ridges to date [5]; topography [8] and gravity data [e.g., 9] provide the means to estimate crustal thickness for the northern hemisphere. We compare these maps to seek relations between crustal thickness and the location and cumulative length of tectonic features.

Pattern of tectonic features: Mercury Dual Imaging System (MDIS) orbital campaigns have provided global monochrome and high-incidence-angle mosaics. Using these mosaics in conjunction with topography from the Mercury Laser Altimeter (MLA) and stereo imaging, a comprehensive global map of prominent large-scale contractional features has been made [5].

Lobate scarps and high-relief ridges are not uniformly distributed across the surface of Mercury. Three longitudinal bands of concentrated features are centered at -110°, -30°, and 120°E; scarps within these bands have a tendency toward north–south orientations. This pattern changes at high latitudes; a latitudinal band of features with dominantly east–west orientations exists south of 60°S, and relatively few large scarps exist north of 60°N [e.g., 5]. Regional-scale zones of weakness appear to control the formation of some lobate scarps and high-relief ridges, such as around basin rims [e.g., 10], along the boundaries between high and low elevation [11], and in assemblages at low elevation and low latitude [5, 12].

Influence of mantle convection: A two-dimensional (2D) viscous flow model of a buoyant crust overlying a zone of mantle downwelling leads to surface horizontal compression and thickening of the crust by as much as a factor of ~1.4, a figure comparable to the degree of crustal thickening beneath an intraplate mountain range in Australia [13].

Axisymmetric simulations of mantle convection on Mercury consistent with constraints on interior structure show that mantle convection likely persisted for a large fraction of Mercury's history [14]. Moreover, variation in surface temperature affects the thickness of the mechanical lithosphere [e.g., 15] and yields fewer convective cells versus latitude than for simulations with a constant surface temperature [14].

Three-dimensional (3D) models of convection on Mercury predict a pattern of long, linear rolls at low latitudes and a hexagonal planform at high latitudes [6]. Such a pattern may account for concentrated bands of tectonic features [6]. However, 3D models to date have not included variable surface temperature or recent constraints on mantle thickness.

Crustal thickness variations: We explore here the possibility that mantle downwelling thickened the overlying crust on Mercury, creating the variation in crustal thickness observed today. Such downwelling would also have enhanced the horizontal compressional stresses at the surface [13] and may have led to a concentration of lobate scarps and high-relief ridges in regions of relatively thick crust.

Methods: In particular, we have explored the relation between the locations of major tectonic features and crustal thickness in the northern hemisphere of Mercury. We compared a crustal thickness map with 0.5° resolution with the locations of lobate scarps and high-relief ridges as mapped by Watters *et al.* [5].

Determining crustal thickness: A crustal thickness map was generated by calculating the crust-mantle interface relief that minimizes Bouguer gravity misfit [16]. We assumed a mean thickness of 20 km (such that the crust has a minimum thickness of zero), a crustal composition intermediate between basaltic and ultramafic (density of 2900 kg m^{-3}), and a 500 kg m^{-3} density contrast at the crust–-mantle interface [17]. We used spherical harmonic terms up to degree and order

50, and we excluded degrees 1 and 2, which show a thickening of the crust toward the equator [9].

The power spectrum of the nominal gravity error surpasses the power of the gravity signal at spherical harmonic degree 35, and gravity and topography data are coherent up to degree 25 [18]. In order to marginalize the erroneous part of the gravity signal we applied a spectral filter that equals 0.5 at degree 35. This filter yields a range of crustal thicknesses from 0 km to 40 km.

Comparison with distribution of tectonic features: The locations of tectonic landforms and crustal thickness were compared within an ArcGIS Mercury project. The centers of all scarp segments in the northern hemisphere were used to extract values from the crustal thickness map.

Results and future work: Lobate scarps occur in regions where the crustal thickness ranges from 10 to 32.5 km (Figure 1a), with a mean of 20.4 km (standard deviation σ_{ls}=4.4 km). This distribution has the same mean value as the full range of crustal thicknesses (Figure 1b) but spans a somewhat smaller range of crustal thickness values. High-relief ridges also occur at the same average crustal thickness (21.2 km, σ_{hrr}=2.6 km) but within the smaller range of 16.8–27.8 km (Figure 1a). The smaller range of crustal thicknesses for high-relief ridges may simply reflect the fewer number of these features than lobate scarps.

The calculated variation in crustal thickness does not indicate that large-scale tectonic features have preferentially formed in regions of thicker crust. There are no preferred crustal thickness values for the localization of either lobate scarps or high-relief ridges. Whereas crustal thickness on Mercury may have been influenced by patterns of mantle convection, via thickening over mantle downwellings, we cannot conclude that mantle convection influenced the localization of tectonic deformation.

A comparison of scarp locations and azimuths to crustal thickness gradients at a variety of wavelengths may yield further insight into how tectonic features are related to crustal thickness. For example, assemblages of tectonic features may preferentially form where the local change in crustal thickness is small [12]. As more information is assembled on the locations and diversity of tectonic features on Mercury, an assessment of the relations explored here should improve our understanding of both the origin of crustal thickness variations and the processes that served to localize large-scale deformation on the innermost planet.

References: [1] Strom R. G. et al. (1975), *J. Geophys. Res. 80*, 2478-2507. [2] Solomon S. C. (1977), *Phys. Earth Planet. Inter. 15*, 135-145. [3] Watters T. R. et al. (2004), *Geophys. Res. Let. 31*, L04701. [4] Watters T. R. et al. (2009), *Earth Planet. Sci. Lett. 285*, 283-296. [5] Watters T. R. et al. (2013), *Lunar Planet. Sci. 44*, this mtg. [6] King S. D. (2008), *Nature Geosci. 1*, 229-232. [7] Solomon S. C. et al. (2001), *Planet. Space Sci. 49*, 1445-1465. [8] Zuber M. T. et al. (2012), *Science 336*, 217-20. [9] Smith D. E. (2012), *Science 336*, 214-217. [10] Fassett C. I. et al. (2012), *J. Geophys. Res. 117*, E00L08. [11] Byrne P. K. et al. (2012), *Lunar Planet. Sci. 43*, 2118. [12] Selvans M. M. et al. (2012), *AGU Fall Mtg.*, P33B-1945. [13] Neil E. A. and Houseman G. A. (1999), *Geophys. J. Inter. 138*, 89-107. [14] Michel N. C. et al. (2013), *J. Geophys. Res.*, *118*, in press. [15] Williams J.-P. et al. (2011), *J. Geophys. Res. 116*, E01008. [16] Wieczorek M. A. and Phillips R. J. (1998), *J. Geophys. Res. 103*, 1715-1724. [17] Nittler L. R. et al. (2011), *Science 333*, 1847-1850. [18] James P. B. et al. (2013), *Lunar Planet. Sci. 44*, this mtg.

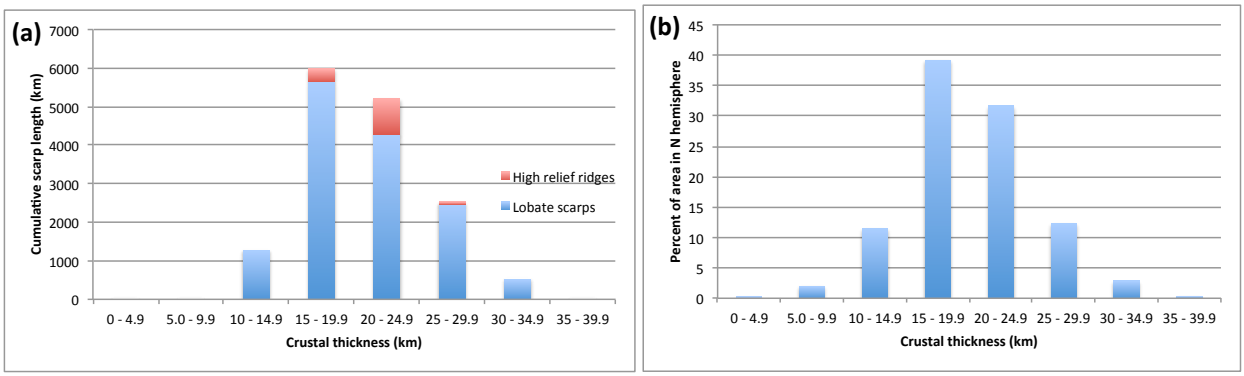

Figure 1. (a) Cumulative length of lobate scarps and high-relief ridges in the northern hemisphere of Mercury within bins of differing crustal thickness. (b) Areal coverage of crustal thickness bins.